16th ICAAR LISBOA 2020-2022

16th International Conference on
Alkali-Aggregate Reaction in Concrete
Lisboa | LNEC | Portugal | 31 May - 2 June 2022

http://icaar2020-2022.lnec.pt

Revisiting the slot-cutting repair technique for facilities affected by AAR using advanced numerical simulations

Mahdi Ben Ftima [(1), (2)], Emre Yildiz [(2)]

(1) Polytechnique Montréal, Montreal, Canada, mahdi.ben-ftima@polymtl.ca

(2) IDAE Consulting Engineers, Montreal, Canada, mahdi.ben-ftima@idae.ca; emre@idae.ca

Abstract

Slot-cutting is a commonly used rehabilitation technique for concrete hydroelectric facilities affected by alkali-aggregate reaction (AAR). Accumulated compressive stresses induced by concrete swelling are released by performing series of saw-cuts at strategic locations. Due to the complexity of AAR phenomenon, results of this rehabilitation technique are not always satisfactory. This work focuses on the development of a rational intervention strategy using the slot-cutting technique by considering advanced simulations. A computational framework developed in previous studies is used to perform multi-physical finite element analysis by considering hydric, thermal and coupled chemo-mechanical processes. A fictitious hydroelectric facility affected by AAR is considered. Several analyses are carried out in order to optimize the location, depth of slot-cutting and re-cutting strategy. Additionally, to the displacement-based performance criteria, a new metric is suggested in this study to represent the amount of cracking. The results showed the potential of intervention strategies involving grouting of slot-cuts.

***Keywords**: slot-cutting; hydroelectric facility; numerical simulation; cracking; repair scenarios*

1. INTRODUCTION

The expansion of the alkali-silica gel, product of alkali-aggregate reaction (AAR) leads to cracking, loss of strength and stiffness at the material level. At the structural level of a hydraulic facility, severe distortion can occur, leading to functional and safety problems. The built-up of compressive stresses introduces differential displacements in weak components (e.g. spillway piers, semi-spiral cases), contributes to gate jamming and even impairs turbine operation. The distortions may also cause important concrete cracking and leakage in gravity dams.

The slot-cutting technique is widely used as a rehabilitation technique for AAR. Reduction of compressive stresses is performed by cutting vertical slots (10 to 30 mm in width) using diamond wire saw, at different locations within the facility. This stress release is accompanied by a short-term elastic rebound and a long-term closure of slot walls due to continuation of AAR and delayed effects ([1],[2]). Additional cracking may also occur in the units adjacent to the slot cut, due to the movement orthogonal to the cutting plane and the increased expansion rate in the direction of tensile stresses. These phenomena are generally difficult to predict using conventional numerical tools such as linear finite elements and equivalent temperature models. It therefore becomes difficult to develop long term scenarios and intervention strategies based on this technique. Slot cuts are generally repeated over time (re-cuts) to compensate for their closures and are more used as remedial and local measures. Furthermore, it is difficult to compare different intervention scenarios, in the absence of performance criteria specific to the context of hydroelectric facilities affected by AAR. Development of reliable advanced simulation tools is therefore a requirement for owners, and it shall ideally be performed in parallel with development of specific quantitative metrics for performance criteria. The combination of these metrics and cost estimates can be used as input in economic analyses to evaluate multiple competing action scenarios or even in optimization algorithms.

Numerous models were suggested in the literature to simulate the complex AAR phenomenon and the effect of slot cutting intervention. Of course, not all the developed approaches are feasible in the context of simulation of large numerical models (overall facility) over several years (say 100 years). Among the models named macro-models, the coupled chemo-mechanical models are of particular interest since they explicitly account for the kinetics of the chemical reaction depending on environmental conditions and consider the anisotropy of swelling depending on the stress state (e.g. [3], [4], [5], [12]). Modelling

of concrete cracking/crushing through a validated non-linear constitutive law is also a requirement to develop useful metrics. Recently, a multi-physical computational framework was developed as a user-subroutine under Abaqus-Explicit and a methodology based on three different finite elements analyses was defined: thermal/hydric analyses and a final nonlinear analysis ([6], [7]). The scope of this work is to consider the developed advanced simulation tools to compare different intervention strategies based on slot-cutting and grouting. A new metric for the assessment of the extent of cracking is suggested, additionally to the conventionally used metrics based on the displacement field. All the simulations are performed on a fictitious hydroelectric facility, developed in previous works.

2. ADVANCED NUMERICAL SIMULATION

2.1 Multi-physical approach

The multi-physical approach uses three different finite element analyses with a sequential coupling ([8]). In a first step, implicit transient hydric and thermal analyses are performed to compute the variation over time of relative humidity field *H(t)* and temperature field *T(t)*. These fields are then imported into a final multi-physical nonlinear finite element analysis involving constitutive concrete model, additionally to the mechanical loads (hydrostatic and gravity loads). The constitutive model is a mechanical concrete model that uses an orthotropic 3D strain-rotating crack model and introduced as a user-subroutine into the software Abaqus-Explicit ([9]). The smeared-cracking approach is used with a very refined mesh in order to capture a reliable cracking pattern. Figure 2.b shows an example of simulated cracking pattern, in which cracked elements are blue colored. This color convention is used throughout this paper. Larive 1998 model [10] is used for the kinetics of the AAR, by defining three main material parameters: the long-term volumetric AAR strain, the latency and characteristic times, which define the 'S-shaped' curve defining the expansion of concrete over time (Figure 2.a). The last two parameters are temperature dependent and therefore ensure the coupling between the temperature field and swelling. The expansion rate and anisotropy are defined by the Saouma and Perotti 2006 model [4] and are dependent on the stress and relative humidity fields.

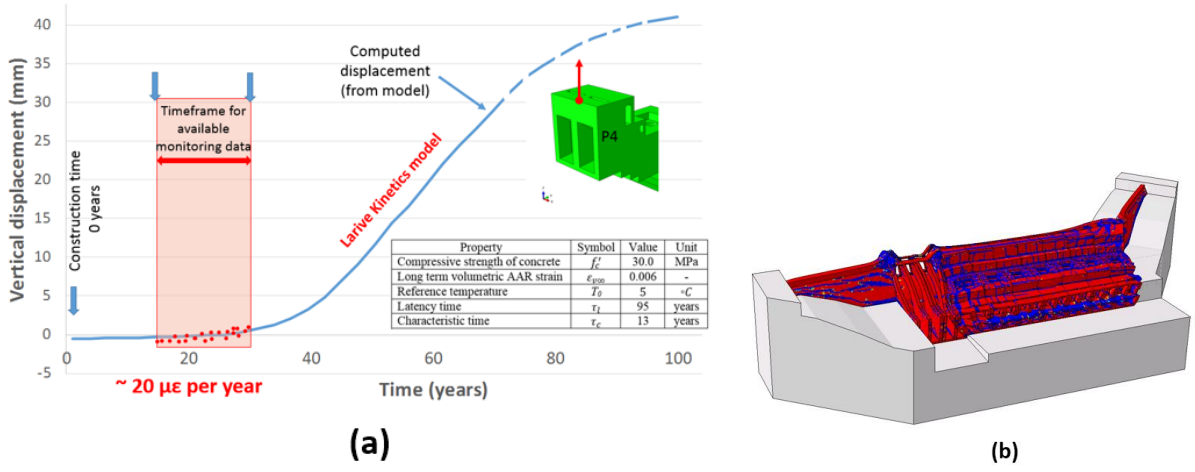

Figure 2.1: Advanced numerical analysis

2.2 Consideration of creep

In the final multi-physical non-linear analysis, the total strain is decomposed into mechanical, thermal creep, shrinkage and AAR strains, according to the following equation in the incremental form:

$$\Delta\epsilon(t,T,H) = \Delta\epsilon_{mec}(t,T,H) + \Delta\epsilon_{th}(t,T) + \Delta\epsilon_{cr}(t,\sigma_0) + \Delta\epsilon_{sh}(t,H) + \Delta\epsilon_{aar}(t,\xi,T,H,\sigma_0) \quad (1)$$

This equation shows the coupling between the four fields considered in the framework: temperature field *T*, relative humidity field *H*, stress field σ_0, and advancement of the chemical AAR reaction field ξ. Both σ_0 and ξ fields are outputs of the final multi-physical nonlinear analysis.

In the previous studies ([6],[7]), only mechanical and AAR strains in Eq.1 were considered. All other strains were neglected. For the purpose of this work, the additional creep strain is considered, and is

based on the recently developed framework ([11]), considering a rheological model for creep, based on the generalized Kelvin chain model. Figure 2.2 shows comparison results with and without considering creep effects. A slight lag effect is seen on the vertical displacement, whereas a relaxation effect can be seen when comparing the cracking pattern with and without creep. It is important to mention here that no explicit reduction was applied on Young's modulus due to AAR effects. This simplification will certainly contribute to minimizing creep effects.

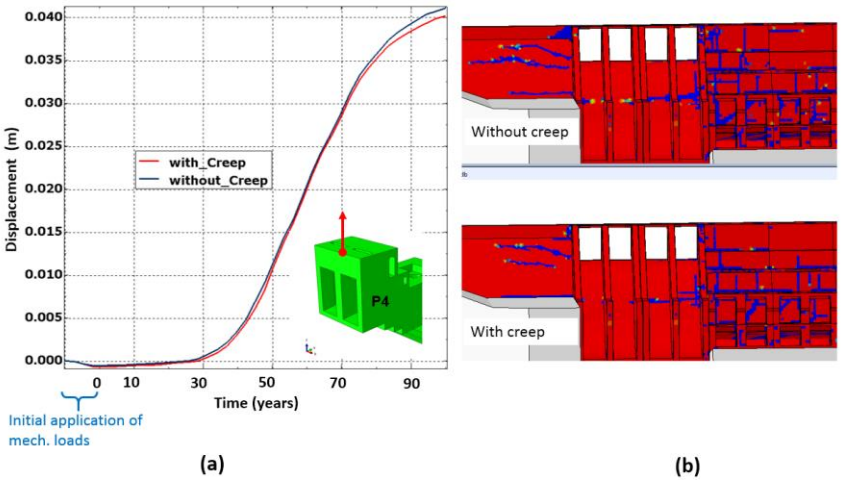

Figure 2.2: Effect of creep: (a) effects on displacement; (b) effects on cracking (t = 60 years)

3. GEOMETRY OF THE FACILITY AND MATERIAL INPUTS

3.1 Geometry and boundary conditions

Figure 3.1 shows the geometry of the fictitious facility along with some dimensions ([6]). The facility with its rock foundation is modeled. It has a total of 11 components (units) with three types: powerhouses (P1 to P7), spillways (S1 to S2) and gravity dams. Mesh refinement is also shown for these typical components. The model has more than 1 million continuum solid elements and more than 2.0 million degrees of freedom. Contact condition is considered between the units (ø = 45°), whereas a full compatibility is assumed at the different concrete/rock interfaces.

The external boundary conditions were fixity condition for the bottom face of the rock and plane strain condition for all the vertical faces of the rock. It was decided to apply the mechanical loads (self weight and hydrostatic loads) quasi-statically at the beginning of the analysis. Relative humidity and temperature fields were imported from the implicit transient analyses. For more details, the reader is referred to reference [6].

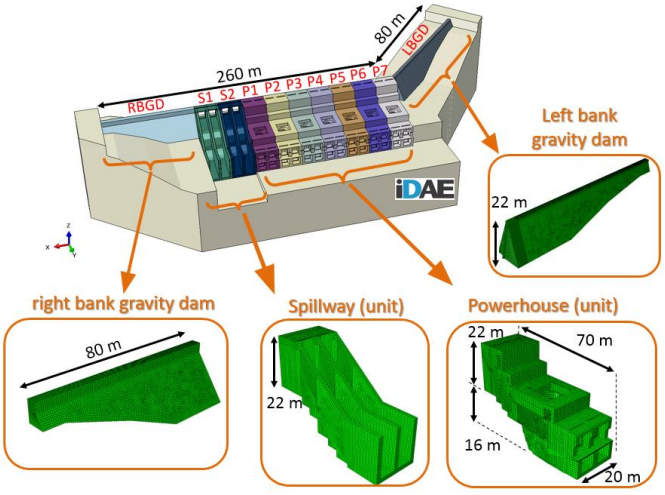

Figure 3.1: Geometry of the facility

3.2 Material inputs

The input parameters for AAR kinetics are shown in Figure 2.1. The fictitious cloud of monitoring data represents a linear slope of 20 $\mu\varepsilon$ per year for the assumed monitoring timeframe (here 15 years from the year 15 to the year 30 which is assumed to be the present year). Monitoring is therefore assumed to start 15 years after the construction of the facility, and this corresponds in the model to the moment when cracking due to AAR becomes visible in the semi-spiral cases. The latency and characteristic times are given in Table 3.1 for a reference temperature of 5$\circ C$ which is a typical average temperature for hydroelectric facilities located in northern Quebec. The activation energies shown in Table 3.1 can be used to find the equivalent latency and characteristic times for other temperatures (e.g. the usual 38°C temperature for accelerated AAR test) using the Arrhenius law. For the mechanical constitutive law, the main input parameter used was the compressive strength of concrete, all other parameters were derived accordingly.

The total period of analysis is 100 years. In Figure 2.2, the year 0 corresponds to the time just after the construction and the impoundment of the facility.

Table 3.1: Input data used for the multi-physical analysis

Property	Symbol	Value	Unit
Mass density of concrete	ρ	2400	kg/m^3
Young's modulus of concrete	E	27500	MPa
Compressive strength of concrete	f_c'	30.0	MPa
Tensile strength of concrete	f_t'	1.8	MPa
Poisson's ratio of concrete	ν	0.18	-
Mode I fracture energy of concrete	G_F	0.15	kN/m
Young's modulus of rock	E	50000	MPa
Poisson's ratio of rock	ν	0.25	-
Long term volumetric AAR strain	$\varepsilon_{v\infty}$	0.006	-
Reference temperature	T_0	5	$\circ C$
Latency time	τ_l	95	years
Characteristic time	τ_c	13	years
Activation energy for characteristic time	U_c	5400	$\circ K$
Activation energy for latency time	U_L	9400	$\circ K$
Compressive limiting stress for AAR	σ_u	10.0	MPa

4. INTERVENTION STRATEGIES AND PERFORMANCE CRITERIA

4.1 Intervention strategies

Analysis of the damage/cracking pattern of the facility conducted in previous studies showed two categories of damage. The first category of local nature is related to the stresses induced from restrained swelling and swelling gradient at the level of each component. The second category is more global at the facility level. It is related to stresses induced by structural discontinuities at the level of the facility: (i) the stiffness discontinuity in the longitudinal axis of the powerhouse units occurring at P1/S2 and S1/RBGD intersections (Figure 4.1) ; and (ii) the geometrical discontinuity due to the angle between the longitudinal axis of the powerhouse units and the longitudinal axis of LBGD.

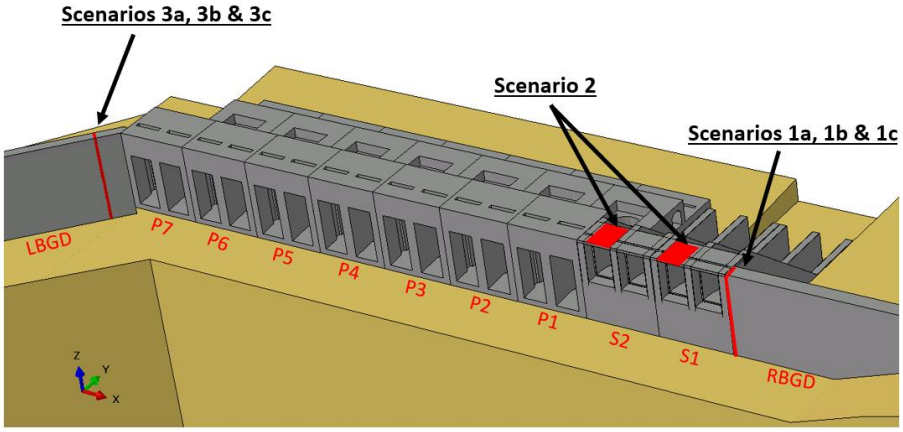

Figure 4.1: Intervention scenarios

Slot-cutting is believed to be more efficient when targeting the second category of damage, due to the global effect of the discontinuities. For this reason, all considered intervention scenarios in this study are selected in the neighbourhood of the discontinuities identified for this facility. In total, seven scenarios are considered in this work (Figure 4.1 and Table 4.1). Scenarios 1a and 3a consider full depth cutting whereas 1b and 3b consider half depth cutting. For all these four scenarios, repetitive re-cuts are required to maintain the opening of the slot walls. Frequencies of the re-cuts shown in Table 4.1 were estimated using initial closure rates from FE analyses. Due to the non-linearity of the swelling curve (Figure 2.1.a), these rates can double over time, thus reducing the frequency of the re-cuts. In scenarios 1c and 3c, grouting is performed into the cut, ten years after the initial slot-cut. In scenario 2, the longitudinal support brought by the spillway bridge is eliminated by removing and replacing the bridge. This remedial measure may be required when crushing of concrete bridge occurs.

Table 4.1: Preliminary input data used for the multi-physical analysis

Repair scenario	Location	Description
Scenario 1a	RBGD/S1	- Full depth slot-cutting at year 30 - Repetitive re-cuts each 16 years*
Scenario 1b	RBGD/S1	- Half depth slot-cutting at year 30 - Repetitive re-cuts each 16 years*
Scenario 1c	RBGD/S1	- Half depth slot-cutting at year 30 - Grouting of the slot-cut at year 40
Scenario 2	S1 & S2	- Removal of spillway bridge
Scenario 3a	LBGD/P7	- Full depth slot-cutting at year 30 - Repetitive re-cuts each 11 years*
Scenario 3b	LBGD/P7	- Half depth slot-cutting at year 30 - Repetitive re-cuts each 11 years*
Scenario 3c	LBGD/P7	- Half depth slot-cutting at year 30 - Grouting of the slot-cut at year 40

* Frequency of the re-cuts assessed using FE models assuming a 25 mm cut

4.2 Performance criteria

Standard performance criteria developed in the literature were generally based on the displacement field output of the FE analyses. The spillway gate closure and the lateral spillway pier displacement are examples of local metrics that can be used for this purpose. As stated in the introduction, these metrics do not allow to benefit from the results of advanced non-linear analyses which additionally allow to capture cracking of the facility nor identify potential failure mechanisms. A new metric is suggested in this study for this purpose, inspired from the cracking index diagnosis method used in industry. The original cracking index method consists in the measurement and summation of crack widths along a set

of lines drawn perpendicularly on the surface of the concrete element investigated, and gives a local assessment of the extent of cracking. This method is known to have some limitations when used with AAR: local assessment of damage and not global, surface and not volumetric cracking, contamination with other surface effects such as freeze and thaw cycles, shrinkage and temperature gradients. Rather than considering a surface cracking, the metric considered in this study, called *TCW* (for total crack width) considers all the volumetric cracking caused by AAR within all elements of a given volume V:

$$TCW(t,V) = \int_{t_0}^{t}(\sum_V(\frac{v_e}{\bar{v}}.h_e.\Delta\varepsilon_{cr-max}))\,dt_0 \quad (2)$$

Where:

- V is the total volume considered (e.g. a unit of the facility or a component of unit);
- $v_e$is the volume of a given mesh element of that volume, h_e is characteristic length of the element;
- $\bar{v}$ is the average volumetric element for all elements in V. For FE model with relatively uniform mesh size, $\frac{v_e}{\bar{v}} \approx 1.0$;
- $\Delta\varepsilon_{cr-max}$ is the principal cracking strain increment occurring in the element, within time increment dt_0.

Hence, *TCW* represents qualitatively the summation of the crack widths over the elements of volume V and is expressed in units of length (e.g. in mm).

TCW can be computed for each unit of the facility for each time. It can also be computed for a particular component of interest within the facility (e.g. spiral cases of all units) or even computed for the overall facility.

5. RESULTS & DISCUSSIONS

5.1 Cracking pattern and TCW

Figures 5.1 to 5.3 present the comparative cracking patterns between the scenarios at the year 60, so 30 years after the initial repair.

The depth of the slot-cut in either scenarios 1 or 3 clearly influences the orientation of the cracks in the adjacent dam (RBGD for scenarios 1, and LBGD for scenarios 3). This understandable phenomenon is linked to the vertical position of the start of the compressive forces, located just below the cut.

Scenario 1c when compared to 1a, 1b and 2 seems to give the least amount of damage to units S2 and P2. On the other side, Scenario 2 is the worst from this point of view, and the excessive lateral deflection of S2 can be clearly noticed from Figure 5.2. According to figures 5.2 and 5.3, all the intervention scenarios appear to result in more cracking if compared to the case with no intervention.

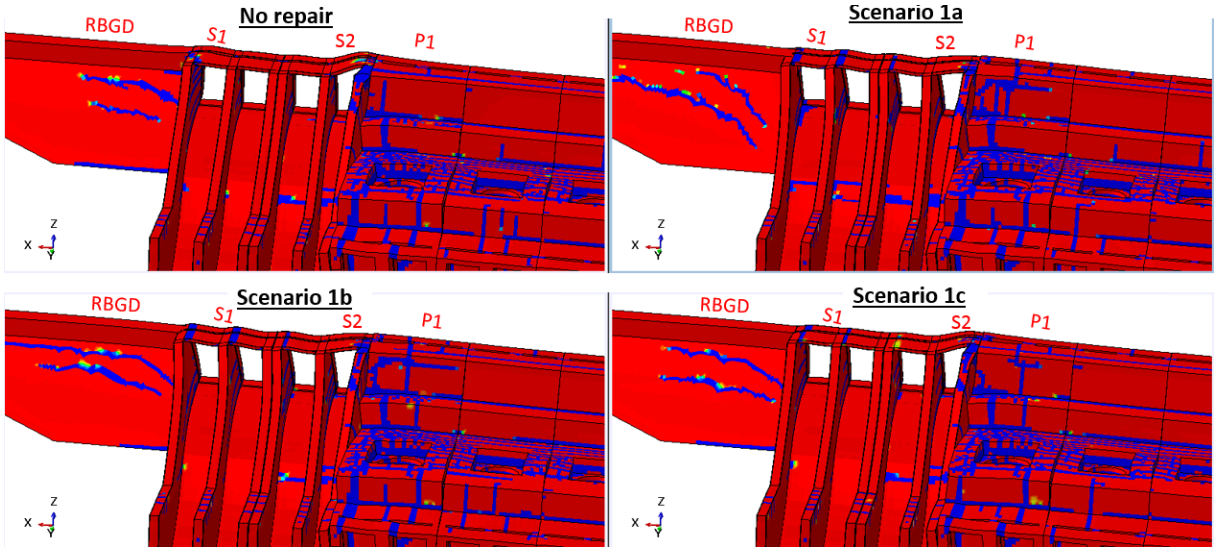

Figure 5.1: Cracking pattern for scenarios 1 (t = 60 years, def. scale x 50)

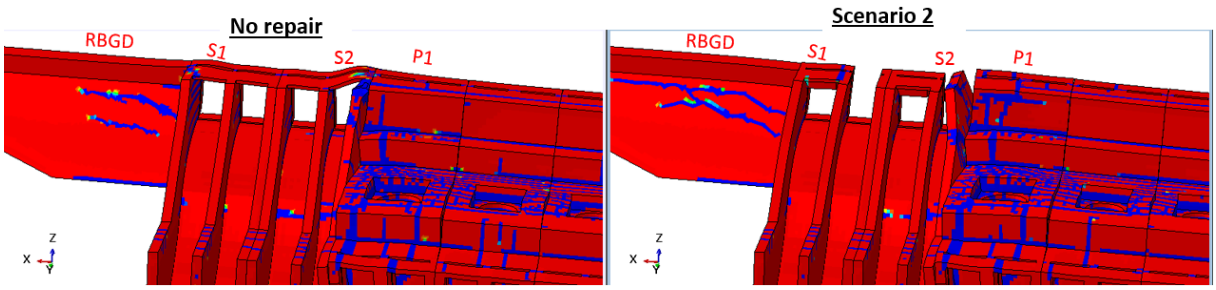

Figure 5.2: Cracking pattern for scenario 2 (t = 60 years, def. scale x 50)

Scenario 3b if compared to repair scenarios 3a and 3c (Figure 5.3) results into more local damage. Examination of FE results actually shows a local failure in the left side intake pier of unit P7 due to location of slot-cut at the mid-depth of LBGD.

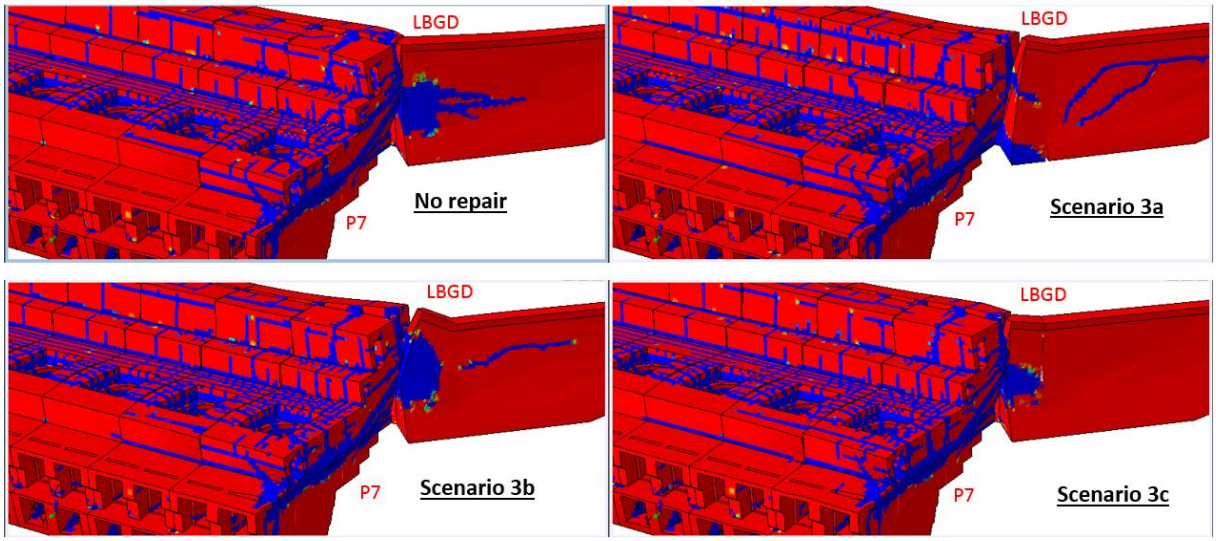

Figure 5.3: Cracking pattern for scenarios 3 (t = 60 years, def. scale x 50)

Comparison of scenarios using visual inspection of cracking pattern is not usually simple. The use of a quantitative metric such as TCW is therefore recommended.

Figure 5.4 shows the computed values of TCW for all the components of the facility, at years 60 and 90.

The first interesting thing to note is the two-peak distribution of all curves. The two peaks are located around the two discontinuities S2/P1 and P7/LBGD. When comparing TCW values for case with no intervention for units P7 and P1 with respect to central unit P4, it can be said that global damage category contributes to 25% to 70% more damage if compared to the local damage category.

It can be seen that effects of a scenario may be beneficial for one component but not beneficial for other components. For example, scenarios 3a, 3b and 3c resulted in less cracking in the LBGD with comparison to the case with no intervention, whereas they produced more cracking in the unit P7 and P6. Table 5.1 gives the best two scenarios for each component of the facility for the years 60 and 90. It is interesting to note that classification doesn't change much with time. By considering all the facility, the best scenarios with respect to the global TCW metric are 3c, 3a and 1c with reductions of 8%, 7% and 2% with respect to the case with no intervention. Scenario 1a was the worst and resulted in an increase of 4% of the global TCW with respect to the case with no intervention. As it will be explained in the next section, this result is linked to a local failure occurring in spillway S1.

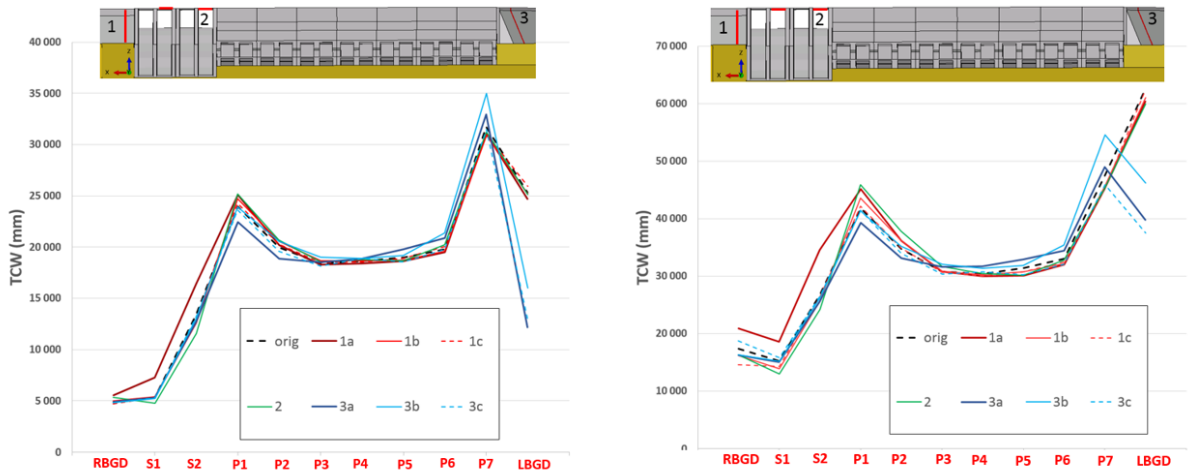

Figure 5.4: Assessment of TCW : (a) t = 60 years; (b) t= 90 years

Table 5.1: Best scenarios in terms of cracking (TCW)

Unit	RBGD	S1	S2	P1	P2	P3	P4	P5	P6	P6	LBGD
Best scenario (t = 60 years)	1c, 3b	2, 3b	2, 1b	3a, 3c	3a, 3c	3c, 3b	1a, 1c	3c, 1a	1a, 1b	1b, 1c	3a, 3c
Best scenario (t = 90 years)	1c, 1b	2, 1b	2, 3a	3a, 3b	3a, 3c	3c, 1c	1a, 1c	1a, 2	1a, 1b	1a, 1b	3c, 3a

5.2 Displacement metrics

Figure 5.5 shows the evolution of lateral displacement of the spillway S2 pier. Scenario 2 resulted in excessive displacement and signs of local failure could be noticed in the simulation model (Figure 5.2).

Scenarios 3a, 3b, 3c and 1c had less impact on the pier displacement.

Figure 5.6.a presents the evolution over time of the spillway S1 gate closure. The closure limit of 25 mm is considered for gate jamming. Due to repetitive re-cuts, jamming is prevented using scenarios 1a and 1b. The same result was also obtained with scenario 2. Repetitive slot-cutting at mid-depth (using scenario 1b) was enough to prevent jamming. Unlike all other repairs, an opening was recorded for scenario 1a. This can be explained by Figure 5.6.b presenting the cracking pattern at year 90. Cutting at full depth resulted in inclined shear cracking at the basis of S1, and more specifically under the right side pier. This adverse effect resulted in an excessive lateral displacement of the right side pier for scenario 1b. Comparing cracking patterns in Figure 5.6.a clearly shows the advantage of slot-cutting at mid-depth for this location.

Interestingly, jamming is delayed by about 25 years using scenario 1c, with respect to the case with no intervention. Also, and as anticipated, scenarios 3a, 3b and 3c had little effects with respect to this perfomance criteria.

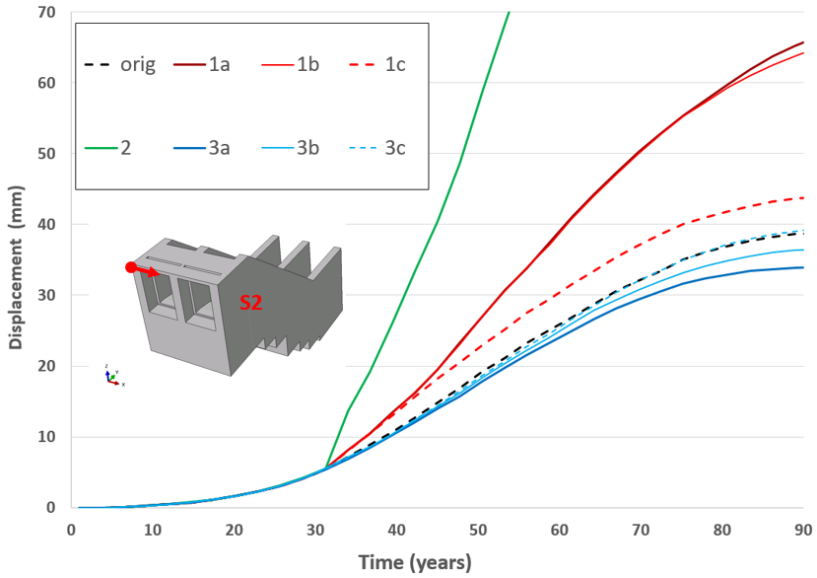

Figure 5.5: Lateral displacement of spillway pier

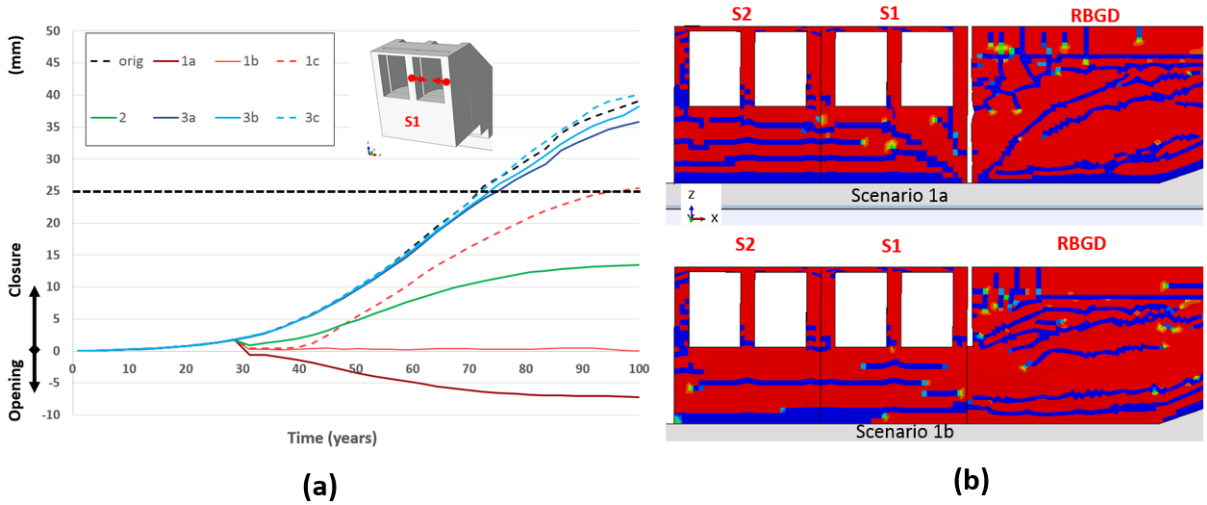

Figure 5.6: Gate closure: (a) evolution over time; (b) cracking pattern (t = 90 years)

5.3 Discussions

When considering all performance criteria, and more specifically the compromise between stress relief, cracking and cost-effectiveness, a combination involving both scenarios 1c and 3c appears to be an interesting starting solution for this facility. Scenario 3c offers the advantage of a generalized stress relief whereas scenario 1c offers the best economical solution for the spillway gate jamming problem.

6. CONCLUSION

Advanced numerical simulation tools were considered in this study to investigate the effects of slot-cutting and compare different repair scenarios. Non-linear simulation is a valuable decision tool, especially when used with quantitative metrics like the TCW metric developed in this study. The authors believe that consideration of performance criteria based only on the displacement field is not representative of the reality of AAR phenomenon. According to this study, grouting of the initial slot-cut, rather than repetitive re-cutting appears to be an interesting solution for hydroelectric facilities affected by AAR. This interesting result shall be confirmed by upcoming studies. The authors believe that the use of advanced numerical tools, combined with specific developed metrics and available cost estimates

can be used for optimizing the location, depth and re-cutting or grouting strategies for a given facility affected by AAR.

7. REFERENCES

[1] Caron, P., Léger, P., Tinawi, R. and Veilleux, M. 2003. “Slot cutting of concrete dams: field observations and complementary experimental studies.”, ACI Structural Journal Vol. 100(4) pp 430–439.

[2] Curtis, D.D, Feng., L., Sooch, G.S, Zheng, Fletcher, J. (2016). Practical analysis and assessment of AAR-affected dams and hydroelectric plants, 36th Annual USSD Conference Denver, Colorado, April 11-15, pp.675-694

[3] Léger, P., Côte, P., and Tinawi, R. 1996. “Finite element analysis of concrete swelling due to alkali-aggregate reactions in dams.”, Computers & Structures, Vol. 60(4) pp 601–611.

[4] Saouma, V., and Perotti, L. 2006. “Constitutive model for alkali aggregate reactions.”, ACI Materials Journal, 103(3) pp194–202.

[5] Sellier, A., Bourdarot, E., Multon, S., Cyr, M. and Grimal, E. 2009. “Combination of structural monitoring and laboratory tests for assessment of alkali aggregate reaction swelling: application to gate structure dam.”, ACI Material Journal; pp 281–290.

[6] Ben Ftima, M. and Yildiz, E. 2018. “Multi-physical simulation of concrete hydroelectric facilities affected by AAR: towards engineering predictive tools.”, CDA Annual Conference, Quebec, Canada, 2018.

[7] Ben Ftima, M., Yildiz, E., Abra, O. (2019). Study of concrete hydroelectric facilities affected by AAR using multi-physical simulation: Consideration of the ultimate limit state. Proceedings, International Commission on Large Dams (ICOLD) 87th Annual meeting, Ottawa, On, Canada, 11 pp.

[8] Ben Ftima, M., Sadouki, H. and Bruhwiler, E. 2016. “Development of a computational multi-physical framework for the use of nonlinear explicit approach in the assessment of concrete structures affected by alkali-aggregate reaction.”, Framcos-9, Berkeley, USA, 2016.

[9] Hibbitt, H.D., Karlson, B.I. and Sorensen, E.P. 2017. ABAQUS version 2017, finite element program. Hibbitt, Karlson and Sorensen, Providence, R.I., USA.

[10] Larive, C. 1998. Apports combinés de l’expérimentation et de la modélisation à la compréhension de l’Alcali-Réaction et de ses effets mécaniques. Thèse, LCPC, Paris.

[11] Ben Ftima, M., Joder, M. And Yildiz, E. (under review). “Creep modelling for multi-physical simulation of mass concrete structures using the explicit finite element approach.”, Submitted to Engineering Structures in september 2019.

[12] Omikrine-Metalssi, O., Seignol, J.-F., Rigobert, S. And Toutlemonde, F. (2014). “Modelling the cracks opening-closing and possible remedial sawing operation of AAR-affected dams”, Engineering Failure Analysis, 36, pp. 199-214.